Synthesis of nickel nanoparticles by reduction of an organometallic precursor with hydrogen

Tibisay del C. Golindano M., Susana I. Martínez M., Omayra Z. Delgado G., y Guaicaipuro P. Rivas R.

Urb. Santa Rosa, Los Teques 1201- Miranda, Venezuela.
PDVSA-INTEVEP.
Tel.(0058)2123306228. Fax:(0058)-2123307139.
martinezsi@pdvsa.com

ABSTRACT

Nanometer sized clusters have received considerable attention in recent decades, because their unique properties, such as quantum size effects, surface and interfacial effects, and other novel phenomena, besides their potential application in industry, for example, catalysis, high-performance ceramics, magnetic recording. In this work, a new method of synthesis of nickel nanoparticles is reported. It has been achieved in an organic solution at the presence of non-ionic surfactant using hydrogen as reductor agent. Nickel nanoparticles of black colour were formed after 8 h. TEM shows a particle size distribution between 1 and 4 nm, with an average value of 2,1 nm. The electron diffraction pattern of nickel evidenced nickel in metallic state with fcc structure and very weak ring, which indicate nickel oxide reflections of cubic face centred (fcc). XPS results showed that the phase layer on Ni nanoparticles is composed of $Ni(OH)_2$.

Keywords: synthesis, nanoparticles, nickel and characterization.

1 INTRODUCTION

With increased interest in fabricating catalysts with nanometric size, much attention has been focused on exploiting a general route to control nanoscale materials size and morphology in synthetic route is indispensable to exploit the properties of this materials [1-7]. In recent years, nanoscale catalytic materials have attracted much interest due to the potential application in the industry. Supported nickel catalysts, comprise one of the most important kinds of heterogeneous catalysts, due to the widespread applications of these systems in a variety of applications, like methanation [8-10], partial oxidation[11,12], and steam reforming [13,14]. A flexible synthetic route is indispensable to exploit catalytic materials. So far, a number of physical and chemical routes have also been applied to produce nanoscale catalytic materials, including as photolytic reduction [15], radiolytic reduction [16], sonochemical method [17], solvent extraction reduction [18], microemulsion technique [19], polyol process [20], and alcohol reduction [21] have been developed for the preparation of metal nanoparticles. For the synthesis of various kinds of metal nanoparticles, some metals such as nickel, copper, and iron are relatively difficult because they are easily oxidized. Nickel nanoparticles have important applications in catalysts and conducting and magnetic materials.. However, the size distribution of the products is not ideal; it appears very difficult to produce particles with sizes in the range of 1-10 nm with relatively good monodispersity. Also, only a few works on the preparation of nickel nanoparticles have been reported up to now. Recent developments of the organometallic route to produce high quality nanocrystals included the thermal decomposition and reduction of organometallic compounds with pure hexadecylamine (HDA) [22] or polyvinylpyrrolidone (PVP) [23] as the stabilizing agents. Within this context, this study presents a new synthesis for to produce nanostructured nickel material with a simple method of preparation.

2 EXPERIMENTAL PROCEDURES

2.1 Preparation of nickel nanoparticles

Typically, an appropriate amount a nickel organometallic precursor (0.1–1 M) and no-ionic surfactant agent were added directly in n-nonane. Then, this mixture was introduced in 300 ml stainless steel autoclave with stirring to appropriate temperature (100-200°C) and hydrogen pressure between 200 and 500 psi. Nickel nanoparticles of black colour were formed after 8 h. The solvent was evaporated under reduced pressure and the solid was washed several times and stored in n-nonane solution, in order to avoid the oxidation. The reduction reaction could be expressed as:

$$(NiR_2) + H_2 \rightarrow Ni^0 + 2RH$$

2.2 Characterization

Transmission Electronic Microscopy (TEM) images were recorded using a Jeol JEM 1200 microscope operated at 100 kV. It provides information from a typical nanometer scale area of the specimen which can moreover be

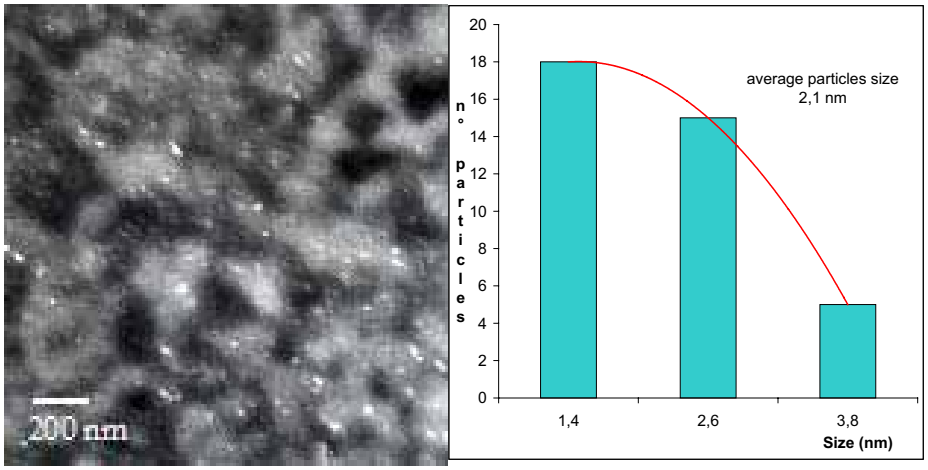

Figure 1: Micrographic and histogram of nickel nanoparticles stabilized with no-ionic surfactan

identified by imaging diffraction modes. Dry Specimens were prepared by depositing one droplet of the particle suspension onto glow-discharged carbon-coated copper grids. After 1 min, the liquid in excess was blotted with filter paper and the remaining film allowed drying. Approximately 100 objects were measured in order to estimate the mean size. Structural information was obtained using selected-area electron diffraction (SAED) patterns.

X-ray photoelectron spectroscopy (XPS) of nanostructure material was performed with a Leybold–Heraeus commercial surface analysis apparatus (LHS 11), equipped with a single channel detector, and employing AlKα radiation (1486.6 eV) at 360W (power settings: 12 kVand 30 mA). The 100 mm radius hemispherical analyzer was set in the constant pass energy mode (pass energy = 200 eV).The normal operating pressure inside the turbo-pumped analysis chamber was kept below 5×10-8 Torr during data collection.
Each spectral region was signal-averaged for a given number of scans to obtain good signal-to-noise ratios. Surface charging was observed on most samples, and accurate binding energies (BE) were determined by charge referencing by means of either adventitious carbon at 284.6 eV or with the reported value for metallic nickel component of 852.3 eV [24]. The nickel particles used for XPS spectral determination were de-agglomerated in n-nonane. Thin layers of particles were added onto a gold plated copper disk. Each added pipet of suspension was given time for the n-nonane to evaporated, until gold substrate was completely coverted.

3 RESULTS AND DISCUSSION

3.1 Microstructural characterization

Figure 1 shows typical dark-field transmission electron micrographs with the corresponding distributions of grain size of the nickel particles. These analysis showed a particle size distribution between 1 and 4 nm, with an average value of 2,1 nm. No coalescence can be detected for these particles. It can be suggested that the no-ionic surfactant might form a protective layer around the particle surface, preventing the aggregation or agglomeration.
The typical electron diffraction pattern of nickel nanoparticles is shown in Figure 2. The pattern evidence that corresponds to nickel in metallic state with fcc structure (d_{111} = 2.02 Å, d_{200} = 1.76 Å, d_{311} = 1.06 Å, d_{222} = 1.02 Å) and very weak ring, which indicate that nickel oxide reflections of cubic face centred (fcc) (d_{111} = 2.41 Å, d_{200}= 2.08 Å, d_{220}= 1.47 Å, d_{311}= 1.26 Å, and d_{222} =1.20 Å) are present.

Figure 2: Electron Diffraction Patterns of nickel nanoparticles

Table 1 shows the theoretical and experimental interplanar diameter, being observed correspondence between them; all Miller Index was corroborated with the literature. The electron diffraction pattern of nickel nanoparticles did not reveals the presence another crystalline phase (carbide or hydroxide). These results indicate that metallic nickel nanoparticles were obtained, but these are not 100 % pure.
The presence of nickel oxidize is probably due to the fact that during the sample preparation, it was exposed to the atmosphere. Due to the presence of this phase the study must be continue with these materials, mainly

improving the conditions of the sample preparation for microscopy.

d_{int} exp. (Å)	d_{int} teoric Ni fcc (Å)	d_{int} teoric NiO fcc (Å)
2.43		2.41
2.09		2.08
2.02	2.02	
1.46		1.47
1.74	1.76	
1.26		1.26
1.20	1.20	1.20
1.06	1.06	
1.02	1.02	

Table 1: Experimental and theory interplanar diameter of metallic and nickel oxide.

3.2 Superficial characterization

Table 2 shows the XPS Ni2p data of the fine nickel particles. Clear Ni2+ peaks (the spectra not shows) are located at binding energies 851 and 873 eV. These peaks corresponds to binding energy measurements in literature for hydroxide nickel[(24)].

Element	Energía de Enlace (eV)
Ni 2p	855.7
O 1s	532.1
N 1s	400.1
C 1s	284.6
Si 2p	102.3

Table 2: XPS Ni2p data of Ni nanoparticles.

Possibly, the layer consists of innermost crystalline NiO, and outermost amorphous $Ni(OH)_2$. XPS indicate that the surface of the particles were completely covered with $Ni(OH)_2$ thin layer. The electron diffraction did not reveal the presence of hydroxide nickel; perhaps due, both the signal overlaps with the nickel oxide signal or this phase of nickel hydroxide is amorphous. But the first reason was discarded, because there isn't correspondence between the Miller Index here reported and the Miller Index of crystalline nickel hydroxide reported in the literature. The carbon presence (table 2) was found to be a contamination possibly from the n-nonane solvent or the XPS high vacuum chamber, and not a carbonaceous product on the Ni particle surface.
In this moment was not possible to determine the degree of oxidation of the nickel nanoparticles.
The structure of the surface layer may be attributed to oxidation and hydration phenomena during the particle exposure to air during material preparation or storage. Due to this, the study must be continue, mainly improving both the conditions of the sample preparation for microscopy and in the synthesis procedure.

4 CONCLUSIONS

The reduction technique of an organometallic precursor with hydrogen was used to synthetisize nickel nanoparticles, which have been characterized to be nickel crystalline of fcc structure converted by both, nickel oxide and hydroxide by TEM and XPS.
The analysis of the sample has showed that this material consists of very small nickel metallic particles, which have an average size of 2.1 nm and a distribution between 1 and 4 nm.
These particles are surrounded by a crystalline surface oxide layer and other phase of $Ni(OH)_2$. XPS showed that there were a superficial $Ni(OH)_2$ layer on the nickel metallic nanoparticles. Was not possible to detect this phase by electron diffraction, because it is amorphous. These results indicate that metallic nanoparticles of nickel were obtained, but these are not 100 % pure.

The quantitative and reproducible chemical approach in organic solvent allows the control of the mean particle size, morphology and stability in organic solvent. Using a relatively simple procedure, it can be applied at low temperature to the synthesis of numerous finely and stable oxides simple or mixed of transition metals which are crucial for industrial applications.

5 ACKNOWLEDGEMENTS

The autors thank the Electron Microscopy service of Universidad Simón Bolívar team, specially Lic. Edgar Cañizales for his support in performing the TEM analysis. Also, we wish to thank specially PhD Gema Gonzalez for making the crystallography and Lic. Juan Carlos de Jesús for his support in performing the XPS.

6 REFERENCES

1. V.F. Puntes, K.M. Krishnan, A.P. Alivisatos, Science 291 (2001) 2115.
2. Pillai, V., Kumar, P., Hou, M. J., Ayyub, P., *Adv. Colloid Interface Sci.* 55**,** 241 (1995).
3. Chahavorty, D., and Giri, A. K., *in* "Chemistry of Advanced Materials" (C. N. R. Rao, Ed.), p. 217. Blackwell Scientific, London, 1993.
4. Henglein, A., *J. Phys. Chem.* 97, 5457 (1993).
5. Benedetti, A., and Fagherazzi, G., *J. Mater. Sci.* 25, 1473 (1990).
6. B. Nagy, J., *Colloids Surf.* 35, 201 (1989).
7. Awschalom, D. D., DiVincenzo, D. P., and Smyth, J. F., *Science* 258, 414
8. M. Agnelli, H.M. Swaan, C. Marquez-Alvarez, G.A. Martin, C. Mirodatos, J. Catal. 175 (1998) 117.
9. A. E. Aksoylu, Z. Onsan, Appl. Catal. A Gen. 164

(1997)1.
10. I. Alstrup, J. Catal. 151 (1995) 216.
11. R. Jin, Y. Chen, W. Li , W. Cui, Y. Ji, C. Yu, Y. Jiang, Appl. Catal.. A Gen. 201 (2000) 71.
12. Z. Liu, K. Jun, H. Roh, S. Baek, S. Park, J. Mol. Catal. A: Chem. 189 (2002) 283.
13. H.S. Bengaard, J.K. Norskov, J. Sehested, B.S. Clauser, L.P. Nielsen, A.M. Molenbroek, J.R. Rostrup-Nielsen, J. Catal. 209 (2002) 365.
14. T. Borowiecki, A. Golebiowski, B. Stasinska, Appl. Catal. A. Gen. 153 (1997) 141.
15. S. Remita, M. Mostafavi, M.O. Delcourt, Radiat. Phys. Chem. 47 (1996) 275.
16. J.H. Hodak, A. Henglein, M. Giersig, G.V. Hartland, J. Phys. Chem. B 104 (2000) 11708.
17. Y. Mizukoshi, K. Okitsu, Y. Maeda, T.A. Yamamoto, R. Oshima, Y. Nagata, J. Phys. Chem. B 101 (1997) 7033.
18. M. Brust, M. Walker, D. Bethell, D.J. Schiffrin, R. Whyman, J. Chem. Soc. Chem. Commun. 801 (1994).
19. K. Osseo-Asare, F.J. Arriagada, Ceram. Trans. 12 (1990) 3.
20 L.K. Kurihara, G.M. Chow, P.E. Schoen, Nanostruct. Mater. 5 (1995) 607.
21. H.H. Huang, X.P. Ni, G.L. Loy, C.H. Chew, K.L. Tan, F.C. Loh, J.F. Deng, G.Q. Xu, Langmuir 12 (1996) 909.16. F.
22. Dumestre, S. Martínez, D. Zitoun, M-C, Fromen, M-J. Casanove, C. Amiens, and B.Chaudret. Faraday Discuss., 125 (2004) 265-278.
23. Dongliang Tao and Fei Wei,. Materials Letters 58(2004)3226-3228.
24. Handbook of X-Ray Photoelectron Spectroscopy, Perkin–Elmer, Eden Prairie, 1978.